Investigating Stability Limits in High Speed Milling of Titanium Thin-Walled Parts

M. Kazemi[1], B. Jabbari Poor [2], B. Moetakef Imani[3], M. H. Sadeghi[4]
[1]Dept. Of Mechanical Engineering, Tarbiat Modares University, Tehran,Iran
[2]Dept. Of Mechanical Engineering, Tarbiat Modares University, Tehran,Iran
[3]Dept. Of Mechanical Engineering, Ferdowsi University, Mashad , Iran
[4]Dept. Of Mechanical Engineering, Tarbiat Modares University, Tehran,Iran

Abstract

The main objective in machining processes is improving the productivity and Efficiency of the process. Nowadays, high speed machining is used to meet the market needs. However, in high speed milling the prediction of stability of machining is the key issue. In this study, the cutting forces for low immersion end-milling are predicted by an efficient dynamic force modeler. In addition, a geometric solid modeler (ACIS) is used in order to model the part, compute the chip load and update the part as the tool removes the material. In this way, the interaction between tool and part is accurately simulated. Finally by using the developed software, the stability of the process is investigated and stability limits are proposed.

Keywords: Stability Limit, Low Immersion Milling, ACIS

2 INTRODUCTION

Maximizing productivity is a primary goal in the machining process. For milling processes, this frequently translates into maximizing the material removal rate (MRR). Possible mechanisms for increasing the MRR include 1) increasing the spindle speed, 2) Increasing the cutting depth, and 3) increasing the feed rate.

In order to decrease the machining cycle and reducing the production time for manufacturing of a main sample its necessary to decrease the time of sequent machining passes or increasing the volume of removal material during the machining passes, which high speed milling(HSM) include both of above mentioned cases.

The high speed milling is vastly used in aerospace industry in order to produce flexible parts of fuselage and it has some advantages in comparing with conventional milling:

1. The main advantage of HSM is presenting gives manufacturers a practical and cost-effective way to produce parts that cannot be as easily produced using standard machining processes.
2. The absence of stress concentrations associated with fastener holes is an added benefit of parts machined out of a single block instead of assembled from many parts.
3. Residual stresses resulting from imprecise assembly are also eliminated.
4. The part's strength and reliability of part can be increased by using HSM techniques.
5. Reduction of weight.
6. Increase of production speed or material removal rate.
7. Reduction of cutting forces.

Examples of these benefits can be found in aircraft parts. These parts are simultaneously lighter, stronger, cheaper, and require a small fraction of the machine time previously needed. [1]

Precise prediction of cutting forces in machining process in order to choose optimum end mill and machine tools are so important. In order to predict problems like chatter or tool damages, at first the value and extent of machining forces should be predicted precisely. With consideration of multi-axis milling, use of presented relations in machining references for calculation of chip load due to complicated geometry is impossible. Also in low immersion cases the variation of contact face due to dynamic tool deflections can not be ignored and in calculation of contact face the edges engagement should be considered. Therefore, in this study the modeling of tool, workpiece, swept volume by tool, tool path and engaged cutting edges with workpiece by means of solid modeling in a precise geometrical modeling software (ACIS) [2] are done. Then the static and dynamic modeling of cutting forces by utilizing force algorithms and ACIS software methods are done and compared with each other, in continuing by means of frequency domain [3] and temporal finite element analysis (TFEA) [4] methods, stability lobes will be obtained and with comparing them the most efficient method for prediction of forces and stable or instable zones in low immersion milling will be identified.

2 TOOL ENGAGEMENT

During milling process the portion of the tool that is engaged with workpiece at a given instant of time is identified as tool engagement. During complex milling operations, usually only a portion of tool engages in cutting and therefore the tool engagement varies along the tool path. The variation in tool engagement results in corresponding variation in the cutting force and a sudden increase in tool engagement may even result in tool breakage. Therefore by identifying tool engagement the cutting forces are determined and can be controlled. Since tool engagement influences cutting forces directly, it has a specific importance [5]. Tool engagement is influenced by the radial and axial depths of cut, because radial and axial depths of cut affect the width and length of the contact area in the feed and rotational directions, respectively. The deeper radial and axial depths of cut, the more flutes will be engaged. Figure 1 shows an illustration of tool engagement during milling. [6]

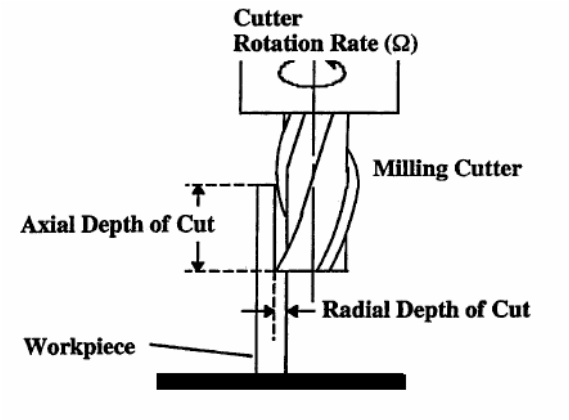

Figure 1: Tool engagement in milling operation. [7]

3 MODELING OF TOOL, WORKPIECE, SWEPT VOLUME BY TOOL, TOOL PATH AND ENGAGED CUTTING EDGES WITH WORKPIECE

In order to calculate the cutting forces it is necessary to estimate the chip dimensions during the machining operations. One of the best devices for obtaining these dimensions is 3-D simulating software. In this software tool and workpiece are engaged with each other through the cutting edges and coordinates of edge engagement are obtained. These coordinates will be used as applicable data for force simulation in next step. In this study a flat end mill with the constant helix angle 30° will be used. For modeling of tool, at first a cylinder with the diameter and height equal to the diameter and cutting length of end mill, respectively, is made. After modeling of cylinder in the software, by utilizing NURBS curve the cutting edge will be modeled. The cutting edge of the tool is illustrated in figure 2.

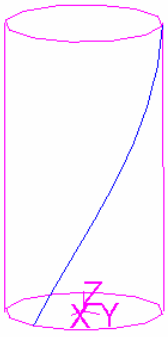

Figure 2: Cutting edge of end mill

The swept volume of the tool is made as following instructions:

Initially two semi-cylinders for the start and end points of the tool path are built. The first semi-cylinder is modeled by means of subtraction of a cube from a cylinder, and then this semi-cylinder is copied and rotated equal to 180° and is transferred to the end of the tool path. This cylinder is rotated in a way, which, the axis of the cylinder is tangent to the tool path. By use of tool path and a surface perpendicular to it the swept volume of tool is constructed. These three volumes (two semi-cylinders and swept volume) are uniformed and finally a solid object that identifies the whole swept volume is modeled. Figure 3 illustrates the swept volume of tool.

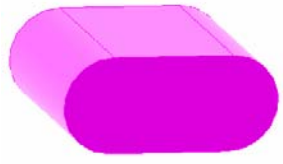

Figure 3: Swept volume of tool

In the next step by means of subtraction of swept volume from workpiece the contact face will be identified. Then the helix edge is transferred to the definite corner of contact face. With rotation of this edge equal to the suitable angular increment (e.g. 0.05° in order to prevent from result divergence) the first and last intersect points of helix edge with the boundaries of contact face in different angular positions can be calculated. In figure 4 the contact face and engaged cutting edges during the execution of ACIS programme, are illustrated.

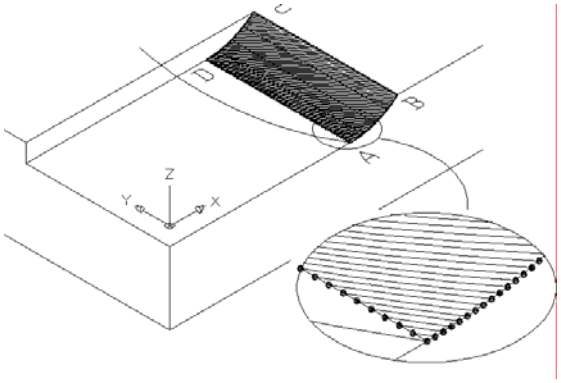

Figure 4: Edge engagement with workpiece

The boundaries AB, BC of the contact face identify the start coordinates of edge engagement and boundaries of CD and DA identify the end coordinates of edge engagement. Modeling and calculations are done by means of ACIS software in the cases of up-milling and down-milling. In down-milling the coordinates of start points begin from A towards B and continue towards C and coordinates of end points begin from A towards D and continue towards C but In up-milling the coordinates of start points begin from C towards B and continue towards A and coordinates of end points begin from C towards D and continue towards A. These above mentioned coordinates are stored in a text file and used in order to calculate static or dynamic forces or for deflection of tool or workpiece. By use of start and end points coordinates of engaged edges with workpiece, the entry and exit angles of edges in workpiece during machining operation are calculated by utilizing following relations:

$$\sin\phi = \frac{x}{r} \Rightarrow \sin\phi_s = \frac{x_s}{r} \Rightarrow \sin^{-1}\frac{x_s}{r}$$
$$\sin\phi_e = \frac{x_e}{r} \Rightarrow \sin^{-1}\frac{x_e}{r} \qquad (1)$$

Using **Matlab V.7** software and entry and exit angles which are obtained from **ACIS** software, a programme for calculation of milling forces in different immersions is written. The obtained results have been compared with force calculation algorithms which are presented in machining references, and it determines that, results of algorithm method and ACIS method are completely equal.

4 LOW IMMERSION

The radial depth of cut plays an important role in milling forces because as the radial depth of cut is increased, the contact area increases in the rotational direction, and the forces become larger. Recent findings indicate that tool wear rates in difficult-to-machine materials (e.g. titanium alloys) decrease significantly as radial immersion is decreased, thus necessitating low radial- immersion machining of flexible workpieces.[7]

Time domain simulation for six machining cases corresponding with table 1 has been done. The results of simulation for offered cases: 1) WOC=1mm and DOC=5mm, 2) WOC=2mm and DOC=5mm, 3) WOC=3mm and DOC=5mm, 4) WOC=1mm and DOC=6mm, 5) WOC=1mm and DOC=7mm, 6) WOC=1mm and DOC=8mm are illustrated in figure 5. In each figure the resultant of cutting forces in x and y directions are presented. In figure 5, it is demonstrated that when the radial depth of cut increases, milling forces increase, since the contact area is increased. Also when the axial depth of cut is increased, the length of engaged flutes increases, and the milling forces increase, But the effect of radial depth of cut in increasing cutting forces is more noticeable than axial depth of cut. In addition, it also shows that the shape of the measured force chart becomes smoother when axial depth of cut increases. This is due to the flute engagement, because when the axial depth of cut is larger, the engaged length is constant.

Axial depth of cut	DOC=5 , 6 , 7 , 8 mm
radial depth of cut	WOC=1 , 2, 3 mm
Average specific cutting coefficient (Ti-6Al-4V)	Ks=1356 (N/mm2)[8]
Number of tooth	N=4
Helix angle	$\beta = 30^\circ$
feedrate	$f_t = 0.05\,mm/tooth$
Tool diameter	D=8 mm

Table 1: parameters used in milling process

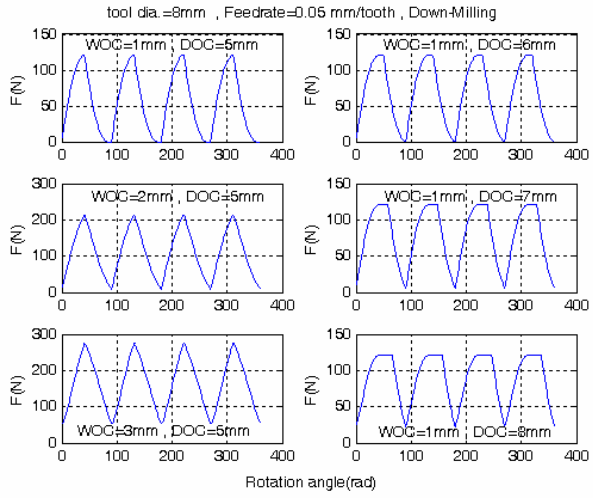

Figure 5: simulated forces with different immersions

5 MATHEMATICAL MODEL OF 2-DOF END MILLING

A schematic diagram of a two-degree-of-freedom milling process is shown in Figure 6.

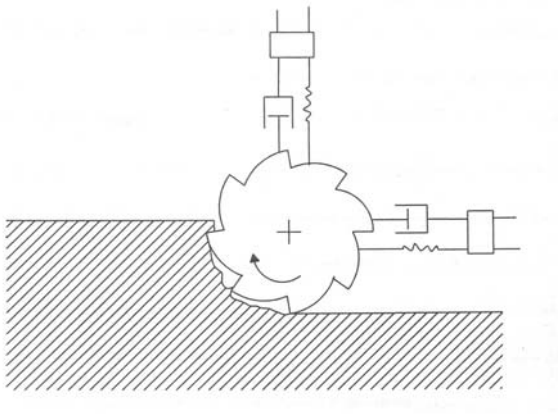

Figure 6: 2-DOF milling model

A tool or structure with a single mode of vibration in two uncoupled and orthogonal directions will result in the following equation of motion: [9]

$$M\ddot{X}(t) + C\dot{X}(t) + KX(t) = F(t) \tag{2}$$

Where $X(t) = [x(t) \;\; y(t)]^T$ is the two-element position vector and M, C, and K are respectively the 2×2 mass, damping, and stiffness matrixes of Equation 2.

The x and y cutting force components on the *P*th tooth are given by:

$$\begin{aligned} F_{xp}(t) &= [-F_{tp}(t)\cos\theta_p(t) - F_{np}(t)\sin\theta_p(t)]g_p(t) \\ F_{yp}(t) &= [F_{tp}(t)\sin\theta_p(t) - F_{np}(t)\cos\theta_p(t)]g_p(t) \end{aligned} \tag{3}$$

Where $g_p(t)$ acts as a switching function, it is equal to one if the *P*th tooth is active and zero if it is not cutting. The tangential and normal cutting force components, F_{tp} and F_{np} respectively, are considered to be the product of linearized cutting coefficients K_t and K_n the nominal depth of cut (DOC) and the instantaneous chip width $w_p(t)$:

$$\begin{aligned} F_{t,p}(t) &= K_t.doc.w_p(t) \\ F_{r,p}(t) &= K_n.doc.w_p(t) \end{aligned} \tag{4}$$

Where $w_p(t)$ depends upon the feed per tooth, f_t, the cutter rotation angle $\theta_p(t)$ and regeneration in the compliant structure directions:

$$\begin{aligned} w_p(t) = f_t \sin\theta_p(t) &+ [x(t) - x(t-\tau)]\sin\theta_p(t) \\ &+ [y(t) - y(t-\tau)]\cos\theta_p(t) \end{aligned} \tag{5}$$

Here, $f_t \sin\theta_p(t)$ is the circular tool path approximation, $\tau = 2\pi / Nn \;[s]$ is the tooth pass period, n is the spindle speed given in rpm and N is the total number of cutting teeth. The angular position of the *P*th tooth for a tool with evenly spaced teeth is:

$$\theta_p(t) = \Omega t + 2\pi(p-1)/N \;,\; p = 1,2,3,.....,N \tag{6}$$

That $\Omega = \frac{2\pi n}{60}$, the total cutting force equations are found by summing the forces on each cutting tooth and substituting Equation 4 and 5 into Equation 3:

$$\begin{bmatrix} F_x \\ F_y \end{bmatrix} = \sum_{p=1}^{N} g_p(t).doc.(f_t \begin{bmatrix} -K_t sc & -K_n s^2 \\ K_t s^2 & -K_n sc \end{bmatrix} + \begin{bmatrix} -K_t sc - K_n s^2 & -K_t c^2 - K_n sc \\ K_t s^2 - K_n sc & K_t sc - K_n c^2 \end{bmatrix} \begin{bmatrix} \Delta x \\ \Delta y \end{bmatrix} \quad (7)$$

Where $s = \sin\theta_p(t)$, $c = \cos\theta_p(t)$ and $\Delta x = x(t) - x(t-\tau)$, $\Delta y = y(t) - y(t-\tau)$,

A more compacted form for the equation of motion is realized by defining the substitutions:

$$f_\circ(t) = \sum_{p=1}^{N} g_p(t) f_t \begin{bmatrix} -K_t sc & -K_n s^2 \\ K_t s^2 & -K_n sc \end{bmatrix} \quad (8)$$

$$K_c(t) = \sum_{p=1}^{N} g_p(t) \begin{bmatrix} -K_t sc - K_n s^2 & -K_t c^2 - K_n sc \\ K_t s^2 - K_n sc & K_t sc - K_n c^2 \end{bmatrix} \quad (9)$$

And rewriting Equation 1 as

$$M\ddot{X}(t) + C\dot{X}(t) + KX(t) = K_c(t).doc.[X(t) - X(t-\tau)] + f_\circ(t).doc \quad (10)$$

$K_c(t)$ and $f_\circ(t)$ are periodic functions with the same period of tool path. Since the cutting stability has been influenced only by the dynamic part of chip thickness therefore in the Equation 10 $f_\circ(t).doc$ term can be ignored and the final vibration equation is presented in following: [10]

$$M\ddot{X}(t) + C\dot{X}(t) + KX(t) = K_c(t).doc.[X(t) - X(t-\tau)] \quad (11)$$

When the structure is only compliant in a single direction, Equation 10 can be modified by eliminating the corresponding rows and columns of the opposing direction. For instance, a structure compliant only in the x direction would have the following equation of motion:

$$\ddot{X}(t) + 2\xi\omega_n\dot{X}(t) + \omega_n^2 X(t) = \frac{K_{sx}(t).doc}{m}[X(t) - X(t-\tau)] \quad (12)$$

Figure 6 presents the specific cutting force variation Ks(t) for different partial immersion up-milling operation by a two fluted tool. The following experimentally identified parameters were used:

$K_t = 5.5\times10^8\, N/m^2$, $K_n = 2\times10^6\, N/m^2$

The discontinuity of the function is due to the tooth passing effect. In the %50 immersion case the entry and exit angles are 0° and 90° respectively. If the angular position of the teeth are $90^\circ < \varphi 1 < 180^\circ$ and $270^\circ < \varphi 2 < 360^\circ$ then both teeth are out of cut and the function *Ks*(*t*) is zero. [11]

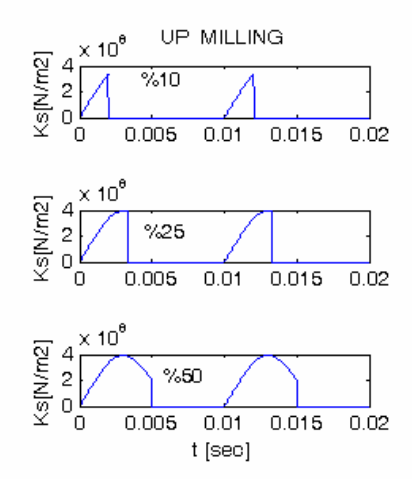

Figure 7: The specific cutting force variation.

6 COMPORISON OF DYNAMIC MODELING OF MILLING FORCES BY USING MILLING FORCES ALGORITHM AND ACIS

By application of **Matlab V.7** software and milling forces algorithms which are presented in machining references and also the coordinates of entry and exit points of engaged cutting edge which are calculated from ACIS, the modeling of force is done. F_X, F_Y, F forces for different immersions by use of two methods are presented.

In order to study frequency analysis and obtaining the dominant frequency in system, the F.F.T chart for resultant force has been shown. With application of parameters in table 2 the results of two methods, for cases of up-milling and down-milling are illustrated in figure 8, figure 9 and figure10.with consideration of figure 8, it is obvious that in stable machining operation, the dominant frequency is the tool path frequency. Tool path frequency can be calculated from following relation:

$$Tool\ Path\ \ Frequency\ \ [HZ] = \frac{nN}{60} \quad (13)$$

In the above relation N and n identify the tooth number and spindle speed respectively.

$f_x = 660\,Hz$ $f_y = 660\,Hz$ $k_x = 2\times10^7\, N/m$ $k_y = 2\times10^7\, N/m$ $\xi_x = 0.05$ $\xi_y = 0.05$	Number of Tooth = 4 Tool diameter = 8mm Feed per tooth = 0.1mm
$K_n = 6.6\times10^8\, N/m^2$	$K_t = 2\times10^9\, N/m^2$

Table 2: cutting conditions and modal parameters using in dynamic simulation

As illustrated in figure 10, by increasing the radial depth of cut as 3 mm, it is obvious that the force amplitude is increased uncontrollably and the system will be instable. Instability is due to domination of chatter frequency to the tool path frequency.

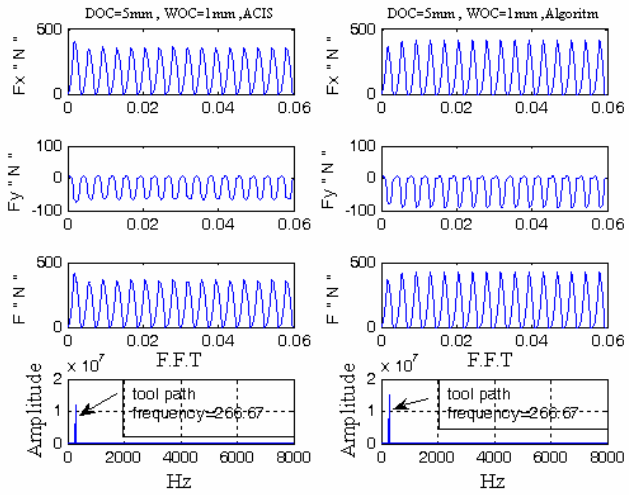

Figure 8: up-milling, axial depth of cut =5 mm, radial depth of cut = 1mm

Two methods: ACIS and force algorithms

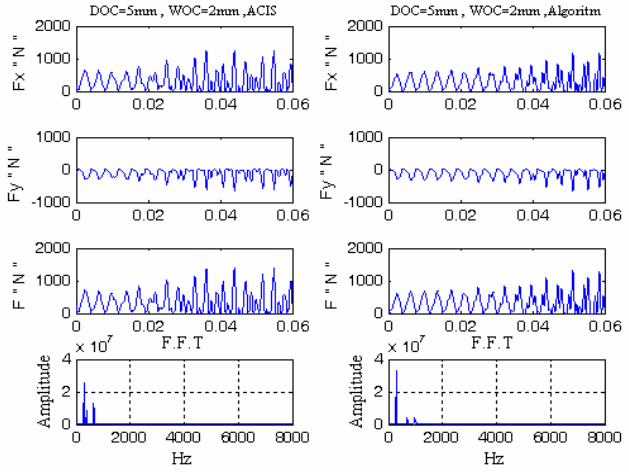

Figure 9: up-milling, axial depth of cut =5 mm, radial depth of cut = 2mm

Two methods: ACIS and force algorithms

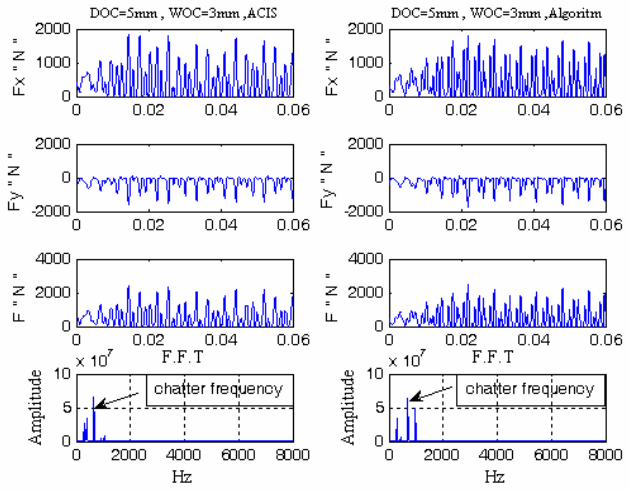

Figure 10: up-milling, axial depth of cut =5 mm, radial depth of cut = 3mm

Two methods: ACIS and force algorithms

7 STABILITY LOBES

Prediction of stability in low immersion milling is complicated by two facts: 1) The equation of motion when cutting is not the same as the equation when the tool is free. 2) No exact analytical solution is known when the tool is in the cut.

The boundary between stable cutting (without chatter) and instable cutting (with chatter) can be illustrated by diagram of axial depth of cut against spindle speed.

By means of stability lobes chart, finding a suitable combination of machining parameters which provide maximum material removal rate without chatter, is possible.

In this part of study, stability charts will be researched. There are two kinds of stability lobes in low immersion milling. In this paper, stability charts in up-milling and down-milling, with different immersions by utilizing frequency domain method and TFEA are obtained. With comparison of charts in different immersions, it will be identified that the most efficient result for estimating the stability lobes can be obtained in low immersion case. Here these methods are concisely explained:

7.1 Calculation of stability lobes by frequency domain method

Frequency domain is a method to obtain the stability lobes for high-speed milling. In this method for obtaining the stability lobes diagram, the transfer function matrix which relates forces and displacements at tool-workpiece contact zone is considered:

$$[\phi(i\omega)] = \begin{bmatrix} \phi_{xx}(i\omega) & \phi_{xy}(i\omega) \\ \phi_{yx}(i\omega) & \phi_{yy}(i\omega) \end{bmatrix} \tag{14}$$

Where Φ*xx(iw)* and Φ*yy(iw)* are the direct transfer functions in the *x* and *y* directions, and Φ*xy(iw)* and Φ*yx(iw)* are the cross transfer functions.

The natural frequency (w), damping factor (ξ) and stiffness of the mechanical system (k) are determined experimentally. Once these values are found, the real Λ_R and the imaginary Λ_I components of the transfer function for a certain chatter frequency can be calculated by using:

$$\Lambda_R = \frac{1-r^2}{K[(1-r^2)^2 + (2\xi r)^2]}$$
$$\Lambda_I = \frac{-2\xi r}{K[(1-r^2)^2 + (2\xi r)^2]} \tag{15}$$

Where $r = \frac{\omega_c}{\omega}$ and ω_c is a chatter frequency.

It is necessary also to consider the average number of teeth during the cut (m):

$$m = \frac{N}{2}\frac{woc}{d} \tag{16}$$

Where d is the tool diameter, N the number of teeth of the tool and WOC the radial depth of cut. The axial depth of cut limit of stability is calculated with the following equation:

$$a_{\lim} = -\frac{1}{2K_m \alpha m \Lambda_R} \tag{17}$$

Where α and Km are directional orientation factor and cutting stiffness, respectively. The phase shift

(ε) between the inner and outer modulations (present and previous vibrations marks) is obtained from the following equation:

$$\varepsilon = 2\pi - (2\cot(\frac{\Lambda_R}{\Lambda_I})) \quad , \quad T = \frac{1}{\omega_c}(\varepsilon + 2k\pi) \tag{18}$$

The proposed method to identify the stability lobes for high-speed milling using a combination between the analytical prediction of chatter and the experimental modal analysis for multi –degree of freedom system s is:

Step 1: Obtain the characteristics of the tool, material to be machined and milling process, and obtain the characteristics of the system using the experimental analysis of the system.

Step 2: Calculate the real and imaginary components of the transfer functions (Λ_R , Λ_I), Equation 15.

Step 3: Select a chatter frequency from the transfer function around a dominant mode.

Step 4: Calculate the critical depth of cut from Equation 17.

Step 5: Calculate the spindle speed from (n = 60/NT) for each stability lobe k = 0, 1, 2 , …

Step 6: Repeat from step 2 by scanning the chatter frequencies. [3]

7.2 TFEA method

In this method, while the tool is out of cut, the system is facing free vibration and during the cutting by dividing time to some temporal elements by means of TFEA method, the vibration of tool is obtained. By utilizing Matlab V.7 software, simulation for obtaining stability lobes is done.[4]

It is necessary to mention that in TFEA method with increasing the immersion (radial depth of cut), the cutting time increases and in order to have convergent answers, the number of elements should be more. [12]

8 PREDICTION OF STABILITY CHARTS

For obtaining the stability charts for a 2-DOF system, two methods of Frequency Domain and Temporal Finite Element Analysis (TFEA) by utilizing given parameters in table 3 are used, and by means of Matlab V.7, simulations for different immersions are done.

$f_x = 922\,Hz$ $f_y = 922\,Hz$ $k_x = 1.34\times10^6\,N/m$ $k_y = 1.34\times10^6\,N/m$ $\xi_x = 0.011$ $\xi_y = 0.011$	Number of Tooth = 2 Tool diameter = 8mm Number of elements = 10,20,30 Feed per tooth = 0.1mm
$K_t = 6\times10^8\,N/m^2$	$K_n = 2\times10^8\,N/m^2$

Table 3: cutting conditions and modal parameters using in stability lobes simulation s

The results of simulation for up-milling with 10%, 25% and 50% immersions are presented in figures 11, 12 and 13. The variation of spindle speed are between 5000 rpm to 25000 rpm and different immersion cases are 10%,25% and 50% and number of elements in TFEA method are 10,20 and 30. For WOC=0.5D (50% radial immersion), both methods yield similar results. As radial depth of cut decreases, the discrepancy between the Frequency Domain method and TFEA stability boundaries grows considerably. The most prominent difference is the additional set of lobes located at the odd integer fractions of twice the dominant eigen frequency, ($2f_t/(2k+1)$). These lobes are predicted only by the TFEA method and correspond to the period doubling (flip) bifurcation which causes periodic chatter. There are two basic reasons for this: First, the TFEA method contains a symbolic calculation that makes the procedure faster. Second, the TFEA method discretizes only the time in the cut.

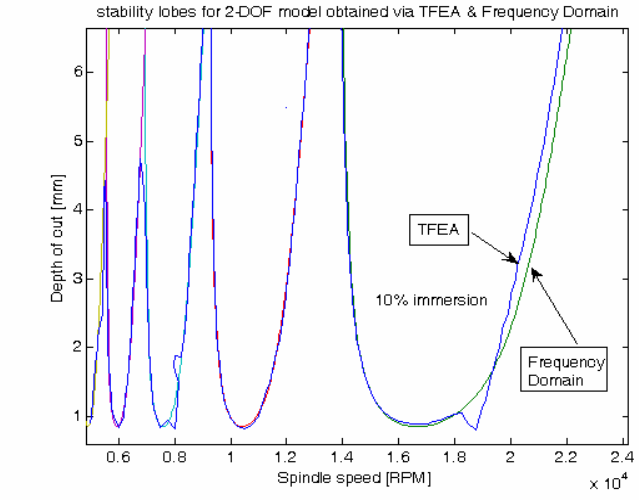

Figure 11: stability lobes chart with two methods in 10% immersion

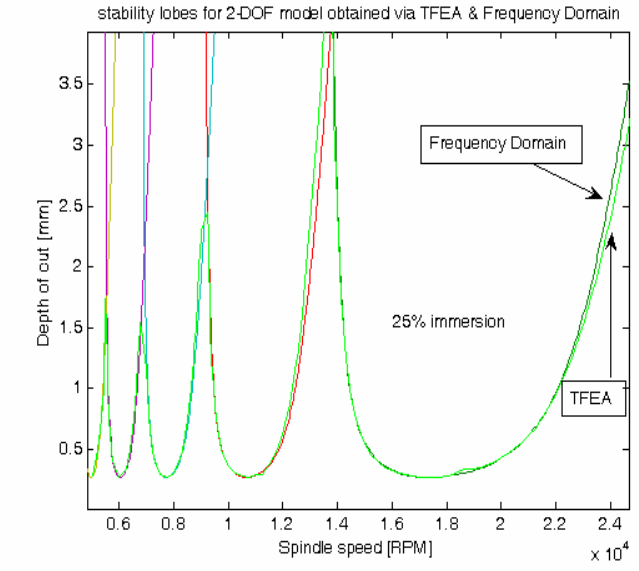

Figure 12: stability lobes chart with two methods in 25% immersion

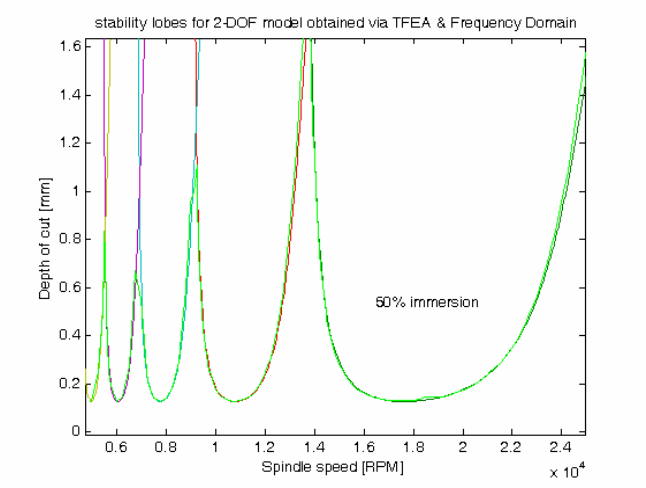

Figure 13: stability lobes chart with two methods in 50% immersion

9 CONCLUSION

Simulation model for end milling process is presented. The tool-workpiece intersection boundaries are evaluated using the geometric models of helical end mill and workpiece. By utilizing start and end points coordinates of engaged edges with workpiece, tool immersion angles are extracted from the geometric model in ACIS software. Cutting forces are predicted and compared with two methods of force algorithms and ACIS, that there was a complete accordance between the results of these two methods. The effects of radial depth of cut and axial depth of cut in cutting forces were studied and evaluated, finally it was identified that radial depth of cut is more effective than axial depth of cut in increasing cutting forces. Stability lobes for up-milling case in various immersions by utilizing frequency domain and TFEA methods are obtained and the most efficient method for analyzing low immersion milling is identified.

10 REFERENCES

[1] Modern Machine Shop 8/99 online supplement: www.mmsonline.com/articles/089903.html

[2] Spatial Technology, Inc., Boulder, Colorado.1994, ACIS Geometric modeler,

[3] E. Solis, C.R. Peres , J.E. Jime´nez, J.R. Alique, J.C. Monje ,2004, A new analytical–experimental method for the identification of stability lobes in high-speed milling, International Journal of Machine Tools & Manufacture 44: 1591–1597

[4] B.P. Mann, P.V. Bayly, M.A. Davies, J.E. Halley, 2004, Limit cycles, bifurcations, and accuracy of the milling process, Journal of Sound and Vibration 277: 31–48

[5]. Satyandr K. Gupta, Sunil K. Saini, Brent W. Spranklin, Zhiyang Yao, 2005, Geometric algorithms for computing cutter engagement functions in 2.5D milling operations Computer-Aided Design 37 : 1469–1480

[6] Wenhsiang Lai, Bryan Green Way, Terry Faddis, 2001, Flute engagement in peripheral milling, Journal of Materials Processing Technology 117:1-8

[7] M. A. DAVIES, B. BALACHANDRAN, Impact dynamics in Milling of Thin-Walled Structures", *Nonlinear Dynamics* 22: 375–392, 2000.

[8] L.N. LoÂpez de lacalle, J. PeÂrez, J.I. Llorente, J.A. SaÂnchez, 2000, Advanced cutting conditions for the milling of aeronautical alloys, Journal of Materials Processing Technology 100 : 1-11

[9] J. Gradi_sek, E. Govekar, I. Grabec, M. Kalveram, K. Weinert,T. Insperger, G. Ste´p_an, 2005, On stability prediction for low radial immersion milling

[10] T. Insperger, B.P. Mann, G. Ste´pa´n, P.V. Bayly, 2003, Stability of up-milling and down-milling, part 1: alternative analytical methods, International Journal of Machine Tools & Manufacture 43: 25–34

[11] Ferenc Hartung, Tama´s Insperger, Ga´bor Ste´pa´n, Janos Turi, 2006, Approximate stability charts for milling processes using semi-discretization, Applied Mathematics and Computation 174: 51–73

[12] P. V. Bayly, J. E. Halley, B. P. Mann, M. A. Davies, 2003, Stability of Interrupted Cutting by Temporal Finite Element Analysis